

Stochastic analysis of pitch angle scattering of charged particles
by transverse magnetic waves

Don S. Lemons*, Kaijun Liu, Dan Winske, and S. Peter Gary

Los Alamos National Laboratory

Los Alamos, New Mexico 87545

Abstract

This paper describes a theory of the velocity space scattering of charged particles in a static magnetic field composed of a uniform background field and a sum of transverse, circularly polarized, magnetic waves. When that sum has many terms the auto-correlation time required for particle orbits to become effectively randomized is small compared to the time required for the particle velocity distribution to change significantly. In this regime the deterministic equations of motion can be transformed into stochastic differential equations of motion. The resulting stochastic velocity space scattering is described, in part, by a pitch angle diffusion rate that is a function of initial pitch angle and properties of the wave spectrum. Numerical solutions of the deterministic equations of motion agree with the theory at all pitch angles, for wave energy densities up to and above the energy density of the uniform field, and for different wave spectral shapes.

*Permanent address: Department of Physics, Bethel College, North Newton, Kansas 67117; email: dlemons@bethelks.edu

I. Introduction

Descriptions of charged particle scattering by magnetospheric, inter-planetary, and cosmic magnetic fields have a long history that has evolved with our ability to measure these particle fluxes and their associated fields [1, 2]. If the magnetic fields are stationary, the scattering is elastic and the velocity of a single particle is confined to a constant energy shell in three-dimensional velocity space. Furthermore, when the average magnetic field does not vanish, it establishes a direction with respect to which the orientation of the particle velocity vector can be described in terms of a pitch angle θ and an azimuthal or phase angle ϕ .

We are primarily concerned in this paper with the pitch angle scattering of high-energy, relativistic electrons trapped in the Earth's magnetic field as these particles interact with low frequency Alfvén/ion-cyclotron waves, also known as EMIC waves [3]. These waves can cause electrons to scatter into their pitch angle loss cone and be absorbed in the earth's atmosphere [4, 5, 6, 7, 8, 9, 10, 11]. Enhanced Alfvén/ion-cyclotron fluctuations are commonly observed in the outer radiation belts of the terrestrial magnetosphere [12, 13, 14] and are produced by a cyclotron instability driven by an ion temperature anisotropy $T_{\perp}/T_{\parallel} > 1$ where here the symbols " \perp " and " \parallel " refer to directions perpendicular and parallel to the average or background magnetic field [15].

High-energy relativistic electrons are sometimes injected into the magnetosphere by magnetic storms [16, 17] and interact strongly with field-aligned Alfvén/ion-cyclotron waves when their speed V and pitch angle θ satisfy the linear resonance condition, that is, $\omega - kV \cos \theta = -\Omega_{oe}$ where $\Omega_{oe} = eB_o/\gamma m_e$ and $\gamma = 1/\sqrt{1 - V^2/c^2}$. Typically, Alfvén/ion-cyclotron wave frequencies ω are so low that $\omega < \Omega_{oi} \ll \Omega_{oe}$ where

$\Omega_{oi} = eB_o/m_i$. In this case the resonance condition reduces to $kV_o \cos\theta \approx \Omega_{oe}$ and the particles interact with effectively static magnetic waves. Put another way: when relativistic electrons interact with Alfvén/ion-cyclotron waves their pitch angles diffuse much more rapidly than their energy. It is for this reason that we limit our analysis to the interaction of charged particles with static magnetic waves.

Most descriptions of pitch angle scattering that are not purely numerical exploit the assumptions of a wave-particle interaction theory variously known as quasi-linear, weak turbulence, and second-order theory [18, 19, 20]. Quasi-linear theory describes the self-consistent interaction of plasma particles with waves generated by the particle distributions by expanding particle orbits around zero-order trajectories. Often this expansion is justified on the basis of small wave amplitudes. Most treatments of fast electron pitch angle scattering by Alfvén/ion-cyclotron waves begin with quasi-linear theory [21, 22, 23, 24].

An alternative method for studying the pitch angle scattering of energetic electrons is to follow test particle dynamics in prescribed waves that are obtained either analytically [25] or from plasma simulation [26]. Then the scattering rates can be obtained directly from test particle data and compared with quasi-linear theory.

Here we outline another approach to wave-particle interaction that uses general statistical methods and does not formally link wave fields to plasma properties. Neither do we explicitly expand particle orbits around zero-order trajectories or limit waves to small amplitudes. Rather, we start with deterministic equations of motion for a charged particle in a given, static, magnetic field, consisting of a uniform background field and transverse, circularly polarized waves, and make only those assumptions necessary to

turn these equations into stochastic differential equations that describe pitch angle scattering. These assumptions – we call them the random variable, the two-time scale, and the random phase assumptions – have a mathematical character whose physical meaning is revealed only after their consequences are derived. In this way we avoid using the wave magnitude as an explicit perturbation parameter. However, a limitation on the relative wave energy density does emerge from the consequences of these assumptions – a limitation that involves not only the wave energy but also the particle pitch angle and other properties of the wave spectrum. For instance, the expression derived for the pitch angle diffusion rate at small pitch angles remains valid even when the wave energy density is many times larger than the energy density in the background field.

We work exclusively with deterministic and stochastic differential equations, rather than with mathematically equivalent kinetic equations, that is, with the Vlasov or Fokker-Planck equations. While the same physical content can be expressed in both of these mathematical languages [27, 28], our assumptions are more easily expressed in terms of differential quantities, and our results more directly compared with numerical solutions of the differential equations solved in test particle simulations.

Because we are concerned with pitch angle scattering by prescribed, stationary, magnetic waves, particle velocities evolve on a constant energy shell in velocity space. Grid-free test particle simulations on this shell are particularly convenient. We use such calculations to illustrate the theory and demonstrate the degree to which the predicted drift and diffusion coefficients are realized. Indeed, these calculations agree with the

theory at all pitch angles, for wave energy densities from 10^{-4} to 10^2 times as large as the energy density in the background field and for different wave spectral shapes.

This paper is organized in the following sections. In Section II we formulate the deterministic equations that define the physics model, while in Section III we apply the three statistical assumptions to the deterministic model equations and in this way turn them into stochastic differential equations. From these we extract particle pitch angle drift and diffusion coefficients that are parameterized by an auto-correlation time -- an expression for which is derived in Section IV. In Section V we investigate the physical limitations that make these results consistent with the assumptions that produce them. We report on numerical test particle simulations that illustrate and verify the theory in Section VI, and finally, in Section VII, we summarize and conclude.

II. Deterministic Model

The equations of motion for a charged particle in a uniform magnetic field $B_0 \hat{x}$ and a transverse magnetic wave field $B_y(x) \hat{y}$ and $B_z(x) \hat{z}$ that depends only upon position x along the direction of the background field are

$$\frac{dV_x}{dt} = V_y \Omega_z - V_z \Omega_y, \quad (1a)$$

$$\frac{dV_y}{dt} = V_z \Omega_x - V_x \Omega_z, \quad (1b)$$

$$\frac{dV_z}{dt} = V_x \Omega_y - V_y \Omega_x, \quad (1c)$$

and

$$\frac{dx}{dt} = V_x \quad (1d)$$

where $\Omega_x = \Omega_o = qB_o/\gamma m$, $\Omega_y = \Omega_y(x) = qB_y(x)/\gamma m$, and $\Omega_z = \Omega_z(x) = qB_z(x)/\gamma m$ are (signed) cyclotron frequencies. Here γ is the Lorentz factor $\gamma = 1/\sqrt{1 - V^2/c^2}$ and V is the speed of the charged particle.

We transform the Cartesian velocity components, V_x , V_y , and V_z , to the spherical polar velocity coordinates V , θ , and ϕ where θ is the particle pitch angle and ϕ is the particle phase angle. The transformation is defined by

$$V_x = V \cos \theta, \quad (2a)$$

$$V_y = V \sin \theta \cos \phi, \quad (2b)$$

and

$$V_z = V \sin \theta \sin \phi. \quad (2c)$$

Equations (2) transform the equations of motion (1) into

$$\frac{d\theta}{dt} = \sin \phi \Omega_y(x) - \cos \phi \Omega_z(x) \quad (3a)$$

$$\frac{d\phi}{dt} = -\Omega_o + \frac{\cos\theta}{\sin\theta} \left[\cos\phi\Omega_y(x) + \sin\phi\Omega_z(x) \right], \quad (3b)$$

and

$$\frac{dV}{dt} = 0. \quad (3c)$$

We choose the transverse field to be a sum of negative helicity [29], circularly polarized waves described by

$$\Omega_y(x) = \sum_k \Omega_k \cos(kx + \alpha_k) \quad (4a)$$

and

$$\Omega_z(x) = \sum_k \Omega_k \sin(kx + \alpha_k) \quad (4b)$$

where α_k is a phase angle associated with wave number k . We shall see that these waves are resonant with electrons moving in the positive direction, that is, in a direction such that $V \cos\theta > 0$.

Combining equations (1d), (3), and (4) produces, after some algebra,

$$\frac{d\theta}{dt} = -\sum_k \Omega_k \sin(kx + \alpha_k - \phi), \quad (5a)$$

$$\frac{d\phi}{dt} = -\Omega_o + \frac{\cos\theta}{\sin\theta} \sum_k \Omega_k \cos(kx + \alpha_k - \phi), \quad (5b)$$

and

$$\frac{dx}{dt} = V_o \cos \theta \quad (5c)$$

where here and subsequently we use V_o to denote the constant particle speed. These are the deterministic equations of motion upon which the rest of this paper is founded.

III. Stochastic Analysis

When the sums in (5a) and (5b) include a large number of waves, equations (5) mimic stochastic differential equations and the variables θ , ϕ , and x mimic random variables. We show this in the following way.

First we formally integrate equations (5a) and (5b) over an interval from t to $t + \Delta t$ so that

$$\Delta\theta = - \int_t^{t+\Delta t} \sum_k \Omega_k \sin(kx + \alpha_k - \phi) dt \quad (6a)$$

and

$$\Delta\phi = -\Omega_o \Delta t + \int_t^{t+\Delta t} \frac{\cos \theta}{\sin \theta} \sum_k \Omega_k \cos(kx + \alpha_k - \phi) dt \quad (6b)$$

where $\Delta\theta = \theta(t + \Delta t) - \theta(t)$ and $\Delta\phi = \phi(t + \Delta t) - \phi(t)$. We now break Δt into n sub-intervals each of duration $\Delta\tau = \Delta t/n$ so that

$$\Delta\theta = - \sum_{i=1}^n \int_{t+(i-1)\Delta\tau}^{t+i\Delta\tau} \sum_k \Omega_k \sin(kx + \alpha_k - \phi) dt \quad (7a)$$

and

$$\Delta\phi = -\Omega_o\Delta t + \sum_{i=1}^n \int_{t+(i-1)\Delta\tau}^{t+i\Delta\tau} \frac{\cos\theta}{\sin\theta} \sum_k \Omega_k \cos(kx + \alpha_k - \phi) dt . \quad (7b)$$

We further rewrite equations (7) in terms of the definitions

$$\Psi_i(t; \Delta\tau) = \int_{t+(i-1)\Delta\tau}^{t+i\Delta\tau} \sum_k \Omega_k \sin(kx + \alpha_k - \phi) dt \quad (8a)$$

and

$$Z_i(t; \Delta\tau) = \int_{t+(i-1)\Delta\tau}^{t+i\Delta\tau} \frac{\cos\theta}{\sin\theta} \sum_k \Omega_k \cos(kx + \alpha_k - \phi) dt \quad (8b)$$

so that equations (7) become

$$\Delta\theta = -\sum_{i=1}^n \Psi_i(t; \Delta\tau) \quad (9a)$$

and

$$\Delta\phi = -\Omega_o\Delta t + \sum_{i=1}^n Z_i(t; \Delta\tau) . \quad (9b)$$

The dimensionless variables $\Psi_i(t; \Delta\tau)$ and $Z_i(t; \Delta\tau)$ are proportional, respectively, to the increment in particle pitch angle θ and phase angle ϕ caused by the magnetic waves during sub-interval i of duration $\Delta\tau$.

Thus far we have merely re-written the deterministic equations (5). In particular, we have made no assumption concerning the size of $\Delta\tau$ relative to the size of Δt other than that $\Delta\tau \leq \Delta t$ since the number of sub-intervals in an interval must be a natural number. Now we are ready to investigate the consequences of the following assumptions.

Random Variable Assumption. We assume that the sub-interval $\Delta\tau$ is large enough that the quantities $\Psi_i(t;\Delta\tau)$ and $Z_i(t;\Delta\tau)$ associated with different sub-intervals are statistically independent random variables. In other words, we assume that the sub-interval $\Delta\tau$ is greater than or equal to an auto-correlation time $\Delta\tau_c$, that is, $\Delta\tau \geq \Delta\tau_c$ where the auto-correlation time $\Delta\tau_c$ is the longest time over which the particle sub-increments remain correlated with each other [30, 31].

Two Time Scale Assumption. We assume that the interval Δt and sub-interval $\Delta\tau$ represent two widely separate time scales -- Δt being an interval over which the dependent variables θ , ϕ , and x change significantly and $\Delta\tau$ being the sub-interval over which the increments $\Psi_i(t;\Delta\tau)$ and $Z_i(t;\Delta\tau)$ become statistically independent random variables. Thus, we assume that the number of sub-intervals $\Delta\tau$ in an interval Δt is a large number $n(= \Delta t/\Delta\tau) \gg 1$. Alternatively, $\Delta\tau(= \Delta t/n) \ll \Delta t$. Since we intend to exploit $n \gg 1$ or, alternatively, $\Delta\tau/\Delta t \ll 1$ we insist on making the two time scales, $\Delta\tau$ and Δt , as widely separated as possible. Therefore, we chose the sub-interval $\Delta\tau$ to be equal to an auto-correlation time $\Delta\tau_c$.

The random variable and two time scale assumptions constrain the auto-correlation time $\Delta\tau_c$ in opposite directions. The former requires that $\Delta\tau_c$ be just large enough that the quantities $\Psi_i(t;\Delta\tau_c)$ and $Z_i(t;\Delta\tau_c)$ associated with different sub-

intervals are statistically independent random variables, while the latter requires that $\Delta\tau_c$ be much smaller than the time Δt required for the dependent variables θ , ϕ , and x to change significantly. Both of these conditions can be met when the number of waves is large. The form of the definitions of $\Psi_i(t;\Delta\tau_c)$ and $Z_i(t;\Delta\tau_c)$ contained in equations (8) suggest as much. In particular, if the variables θ and ϕ change very little during an auto-correlation time $\Delta\tau_c$, the sums on the right hand side of (8) must be over many waves in order that different sub-increments be statistically independent, random variables.

Given that $n \gg 1$ and that the moments of the statistically independent random increments $\Psi_i(t;\Delta\tau_c)$ and $Z_i(t;\Delta\tau_c)$ are finite, as is required since these are proportional to bounded angles, the sums on the right hand side of equations (9) satisfy the conditions of the central limit theorem [32, 33]. Accordingly, this sum approaches, in the limit of a large number of statistically independent addends, a normal random variable with mean and variance equal, respectively, to the sum of the means and variances of the addends. Accordingly,

$$\Delta\theta = -N_{\theta,t} \left[\sum_{i=1}^n \text{mean}\{\Psi_i(t;\Delta\tau_c)\}, \sum_{i=1}^n \text{var}\{\Psi_i(t;\Delta\tau_c)\} \right] \quad (10a)$$

and

$$\Delta\phi = -\Omega_o\Delta t + N_{\phi,t} \left[\sum_{i=1}^n \text{mean}\{Z_i(t;\Delta\tau_c)\}, \sum_{i=1}^n \text{var}\{Z_i(t;\Delta\tau_c)\} \right] \quad (10b)$$

where, for example, the notation $N_{\theta,t}[(...),(...)]$ indicates a normal random variable with mean equal to its first argument and variance equal to its second argument. The

subscripts θ and t indicate that this normal random variable is statistically independent of normal random variables notated with other dependent variables and different times t .

Since, according to the two time scale approximation, the dependent variables θ , ϕ , and x change very little during an autocorrelation time $\Delta\tau_C$, we may expand the integrations in (8) defining $\Psi_i(t; \Delta\tau_C)$ and $Z_i(t; \Delta\tau_C)$ around their value at the beginning of each sub-interval in terms of small auto-correlation time $\Delta\tau_C$. Accordingly, through second order in $\Delta\tau_C$,

$$\Psi_i(t; \Delta\tau_C) = \Delta\tau_C \sum_k \Omega_k \sin(kx + \alpha_k - \phi) - \frac{\Delta\tau_C^2}{2} \sum_k \Omega_k \cos(kx + \alpha_k - \phi) \left(k \frac{dx}{dt} - \frac{d\phi}{dt} \right) \quad (11a)$$

and

$$\begin{aligned} Z_i(t; \Delta\tau_C) = & \Delta\tau_C \frac{\cos\theta}{\sin\theta} \sum_k \Omega_k \cos(kx + \alpha_k - \phi) - \frac{\Delta\tau_C^2}{2 \sin^2\theta} \sum_k \Omega_k \left(\frac{d\theta}{dt} \right) \cos(kx + \alpha_k - \phi) \\ & - \frac{\Delta\tau_C^2}{2} \frac{\cos\theta}{\sin\theta} \sum_k \Omega_k \sin(kx + \alpha_k - \phi) \left(k \frac{dx}{dt} - \frac{d\phi}{dt} \right) \end{aligned} \quad (11b)$$

where the dependent variables θ , ϕ , and x and their time derivatives on the right hand sides of (11a) and (11b) are evaluated at the beginning of each sub-interval i , that is, at time $t + \Delta\tau_C(i-1)$. Given equations (5) we find that

$$k \frac{dx}{dt} - \frac{d\phi}{dt} = kV_o \cos \theta + \Omega_o - \frac{\cos \theta}{\sin \theta} \sum_{k'} \Omega_{k'} \cos(k'x + \alpha_{k'} - \phi) . \quad (12)$$

Substituting the right hand sides of equations (5a) and (12) into equations (11) produces

$$\begin{aligned} \Psi_i(t; \Delta\tau_C) &= \Delta\tau_C \sum_k \Omega_k \sin(kx + \alpha_k - \phi) \\ &\quad - \frac{\Delta\tau_C^2}{2} \sum_k \Omega_k \cos(kx + \alpha_k - \phi) \left(kV_o \cos \theta + \Omega_o - \frac{\cos \theta}{\sin \theta} \sum_{k'} \Omega_{k'} \cos(k'x + \alpha_{k'} - \phi) \right) \end{aligned} \quad (13a)$$

and

$$\begin{aligned} Z_i(t; \tau_C) &= \Delta\tau_C \frac{\cos \theta}{\sin \theta} \sum_k \Omega_k \cos(kx + \alpha_k - \phi) \\ &\quad + \frac{\Delta\tau_C^2}{2 \sin^2 \theta} \left\{ \sum_{k'} \Omega_{k'} \sin(k'x + \alpha_{k'} - \phi) \right\} \sum_k \Omega_k \cos(kx + \alpha_k - \phi) \\ &\quad - \frac{\Delta\tau_C^2}{2} \frac{\cos \theta}{\sin \theta} \sum_k \Omega_k \sin(kx + \alpha_k - \phi) \left\{ kV_o \cos \theta + \Omega_o - \frac{\cos \theta}{\sin \theta} \sum_{k'} \Omega_{k'} \cos(k'x + \alpha_{k'} - \phi) \right\} . \end{aligned} \quad (13b)$$

Random Phase Approximation. In order to calculate the mean and variance of the random variables $\Psi_i(t; \Delta\tau_C)$ and $Z_i(t; \Delta\tau_C)$ we assume that the wave phase factors $kx + \alpha_k - \phi$ are uniform random variables defined on the interval $[0, 2\pi]$. Recall that the mean and variance of any variable A is given, respectively, by $\langle A \rangle$ and by $\langle A^2 \rangle - \langle A \rangle^2$ where the bracket $\langle \dots \rangle$ indicates an average over an ensemble of possible values of its

argument each weighted with a probability. The meaning of this average is defined by the following thought experiment.

Imagine performing an indefinitely large number of experimental trials. In each trial the charged particle is initialized with the same pitch angle $\theta[t + (i-1)\Delta\tau_c]$ in the same magnetic field. The initial particle position $x[t + (i-1)\Delta\tau_c]$ and phase angle $\phi[t + (i-1)\Delta\tau_c]$ are uncontrolled random variables in these experimental trials subject to the random phase approximation, that is, subject to the requirement that the phase $kx + \alpha_k - \phi$ is uniformly distributed on the interval $[0, 2\pi]$. The particle coordinates are then allowed to evolve for a correlation time $\Delta\tau_c$ and the random variables $\Psi_i(t; \Delta\tau_c)$ and $Z_i(t; \Delta\tau_c)$ measured. These random variables are distributed over the interval $[0, 2\pi]$ each value of which is associated with a probability that is constructed from the relative frequencies of the values of $\Psi_i(t; \Delta\tau_c)$ and $Z_i(t; \Delta\tau_c)$ realized in the experimental trials. Note that the initial pitch angle $\theta[t + (i-1)\Delta\tau_c]$ or, more briefly, θ is a given, that is, an initial, sure value in these experimental trials.

The following are consequences of the random phase approximation and this definition of the bracket average: $\langle \cos(kx + \alpha_k - \phi) \rangle = 0$, $\langle \sin(kx + \alpha_k - \phi) \rangle = 0$,
 $\langle \cos(kx + \alpha_k - \phi) \sin(kx + \alpha_k - \phi) \rangle = 0$, $\langle \cos(kx + \alpha_k - \phi) \cos(k'x + \alpha_{k'} - \phi) \rangle = \delta_{k,k'}/2$,
 $\langle \sin(kx + \alpha_k - \phi) \sin(k'x + \alpha_{k'} - \phi) \rangle = \delta_{k,k'}/2$, and
 $\langle f(kx + \alpha_k - \phi) g(\theta) \rangle = \langle f(kx + \alpha_k - \phi) \rangle g(\theta)$ where $f(kx + \alpha_k - \phi)$ is any function of the random phase variable $kx + \alpha_k - \phi$ and $g(\theta)$ is any function of the sure variable θ .

We find, after some algebra, that, through second order in $\Delta\tau_c$:

$$\text{mean}\{\Psi_i(t;\Delta\tau_C)\} = \frac{\cos\theta}{\sin\theta} \frac{\Delta\tau_C^2}{4} \sum_k \Omega_k^2, \quad (14a)$$

$$\text{var}\{\Psi_i(t;\Delta\tau_C)\} = \frac{\Delta\tau_C^2}{2} \sum_k \Omega_k^2, \quad (14b)$$

$$\text{mean}\{Z_i(t;\Delta\tau_C)\} = 0, \quad (14c)$$

and

$$\text{var}\{Z_i(t;\Delta\tau_C)\} = \frac{\cos^2\theta}{\sin^2\theta} \frac{\Delta\tau_C^2}{2} \sum_k \Omega_k^2. \quad (14d)$$

Note that the mean and variance of $\Psi_i(t;\Delta\tau_C)$ and $Z_i(t;\Delta\tau_C)$, as displayed in these equations, are independent of sub-increment index i although they remain implicit functions of the time t through the dependence of θ and $\Delta\tau_C$ on time t .

This latter property allows us to further simplify the sums on the right hand side of (10). In particular, we insert expressions (14) for the mean and variance of $\Psi_i(t;\Delta\tau_C)$ and $Z_i(t;\Delta\tau_C)$, complete the indicated sums, and use $n = \Delta t/\Delta\tau_C$. Then equations (10) become

$$\begin{aligned}
\Delta\theta &= N_{\theta,t} \left[\frac{\cos\theta}{\sin\theta} \frac{n\Delta\tau_c^2}{4} \sum_k \Omega_k^2, \frac{n\Delta\tau_c^2}{2} \sum_k \Omega_k^2 \right] \\
&= N_{\theta,t} \left[\frac{\cos\theta}{\sin\theta} \frac{\Delta\tau_c \Delta t}{4} \sum_k \Omega_k^2, \frac{\Delta\tau_c \Delta t}{2} \sum_k \Omega_k^2 \right] \\
&= \frac{\cos\theta}{\sin\theta} \frac{\Delta\tau_c \Delta t}{4} \sum_k \Omega_k^2 + \sqrt{\frac{\Delta\tau_c \Delta t}{2} \sum_k \Omega_k^2} N_{\theta,t}[0,1]
\end{aligned} \tag{15a}$$

and

$$\begin{aligned}
\Delta\phi &= -\Omega_o \Delta t + \frac{\cos\theta}{\sin\theta} N_{\phi,t} \left[0, \frac{\Delta\tau_c^2 n}{2} \sum_k \Omega_k^2 \right] \\
&= -\Omega_o \Delta t + \frac{\cos\theta}{\sin\theta} N_{\phi,t} \left[0, \frac{\Delta\tau_c \Delta t}{2} \sum_k \Omega_k^2 \right] \\
&= -\Omega_o \Delta t + \sqrt{\frac{\cos^2\theta}{\sin^2\theta} \frac{\Delta\tau_c \Delta t}{2} \sum_k \Omega_k^2} N_{\phi,t}[0,1]
\end{aligned} \tag{15b}$$

where, again, the random variables $N_{\theta,t}(0,1)$ and $N_{\phi,t}(0,1)$ are, for different values of their subscripts, statistically independent unit normals.

For clarity, we rewrite the stochastic equations of motion (15) in differential form, that is, we replace the interval Δt by its equivalent dt , since the time scale quantified by t is the only time scale that remains manifest. Then equations (15) become

$$d\theta = \frac{\Delta\tau_c}{4} \frac{\cos\theta}{\sin\theta} \sum_k \Omega_k^2 dt + \sqrt{\frac{\Delta\tau_c}{2} \sum_k \Omega_k^2} dt N_{\theta,t}(0,1) \tag{16a}$$

and

$$d\phi = -\Omega_o dt + \sqrt{\frac{\Delta\tau_c \cos^2 \theta}{2 \sin^2 \theta} \sum_k \Omega_k^2 dt} N_{\phi,t}(0,1) . \quad (16b)$$

A similar process leaves the third equation

$$dx = V_o \cos \theta dt \quad (16c)$$

unchanged. Equations (16) are the stochastic differential equations that mimic the deterministic equations (5) when all three assumptions, random variable, two-time scale, and random phase, are justified.

IV. Auto-Correlation Time, Drift Rate, and Diffusion Rate

The stochastic differential equation of motion for the pitch angle (16a) assumes the form $d\theta = Cdt + \sqrt{Ddt} N_{\theta,t}(0,1)$ where C is the pitch angle drift rate and D is the pitch angle diffusion rate. Accordingly, these are

$$C = \frac{\Delta\tau_c \cos \theta}{4 \sin \theta} \sum_k \Omega_k^2 \quad (17a)$$

and

$$D = \frac{\Delta\tau_c}{2} \sum_k \Omega_k^2 . \quad (17)$$

That C and D are related by $C = (\cos\theta/\sin\theta)(D/2)$ is an expression of the fluctuation-dissipation theorem [34] applied to this system.

Because the auto-correlation time $\Delta\tau_C$ in expressions (17) may depend, in possibly complicated ways, upon the dependent variables θ , ϕ , and x , the amplitude Ω_o , and the spectrum of amplitudes Ω_k , the simplicity of (17) is only apparent. We use the following argument in order to determine the dependence of $\Delta\tau_C$ on these variables.

Recall that the auto-correlation time $\Delta\tau_C$ must be large enough to make $\Psi_i(t; \Delta\tau_C)$ and $Z_i(t; \Delta\tau_C)$ with different indices i statistically independent but small enough so that the dependent variables θ , ϕ , and x do not change significantly during an auto-correlation time. Thus, for instance, $\Delta\tau_C$ must be such as to render

$$\Psi_i(\Delta t_C; \Delta\tau_C) = \sum_k \Omega_k \int_{t+(i-1)\Delta\tau_C}^{t+i\Delta\tau_C} \sin(kx + \alpha_k - \phi) dt \quad (18a)$$

and

$$\Psi_{i+1}(t; \Delta\tau_C) = \sum_k \Omega_k \int_{t+i\Delta\tau_C}^{t+(i+1)\Delta\tau_C} \sin(kx + \alpha_k - \phi) dt \quad (18b)$$

statistically independent random variables at all times t . A necessary condition for their statistical independence is

$$\langle \Psi_i(t; \Delta\tau_C) \Psi_{i+1}(t; \Delta\tau_C) \rangle = \langle \Psi_i(t; \Delta\tau_C) \rangle \langle \Psi_{i+1}(t; \Delta\tau_C) \rangle. \quad (19a)$$

Given that $\langle \Psi_i(t; \Delta\tau_C) \rangle$ is independent of sub-interval index i , condition (19a) reduces to

$$\langle \Psi_i(t; \Delta\tau_C) \Psi_{i+1}(t; \Delta\tau_C) \rangle = \langle \Psi_i(t; \Delta\tau_C) \rangle^2. \quad (19b)$$

Transforming the integration variable of (18b) from t to $t + \Delta\tau_C$ transforms (18b) to its equivalent

$$\begin{aligned} \Psi_{i+1}(t, \Delta\tau_C) = & \sum_k \Omega_k \int_{t+(i-1)\Delta\tau_C}^{t+i\Delta\tau_C} \{ \sin(kx + \alpha_k - \phi) \cos(k\Delta x - \Delta\phi) \} dt \\ & + \sum_k \Omega_k \int_{t+(i-1)\Delta\tau_C}^{t+i\Delta\tau_C} \{ \cos(kx + \alpha_k - \phi) \sin(k\Delta x - \Delta\phi) \} dt \end{aligned} \quad (20)$$

where here $\Delta x = x(t + \Delta\tau_C) - x(t)$ and $\Delta\phi = \phi(t + \Delta\tau_C) - \phi(t)$. Since the two-time scale assumption requires that the dependent variables shift very little during an auto-correlation time $\Delta\tau_C$, $k\Delta x - \Delta\phi \ll 1$ and we may expand the right hand side of (20) so that it becomes

$$\begin{aligned} \Psi_{i+1}(t; \Delta\tau_C) = & \sum_k \Omega_k \int_{t+(i-1)\Delta\tau_C}^{t+i\Delta\tau_C} \left(1 - \frac{(k\Delta x - \Delta\phi)^2}{2} \right) \sin(kx + \alpha_k - \phi) dt \\ & + \sum_k \Omega_k \int_{t+(i-1)\Delta\tau_C}^{t+i\Delta\tau_C} (k\Delta x - \Delta\phi) \cos(kx + \alpha_k - \phi) dt. \end{aligned} \quad (21)$$

We now form the product of $\Psi_i(t; \Delta\tau_C)$ and $\Psi_{i+1}(t; \Delta\tau_C)$

$$\begin{aligned}
\Psi_i(t; \Delta\tau_C) \Psi_{i+1}(t; \Delta\tau_C) = & \\
& \sum_{k'} \Omega_{k'} \int_{t+(i-1)\Delta\tau_C}^{t+i\Delta\tau_C} \sin(k'x + \alpha_{k'} - \phi) dt \sum_k \Omega_k \int_{t+(i-1)\Delta\tau_C}^{t+i\Delta\tau_C} \left(1 - \frac{(k\Delta x - \Delta\phi)^2}{2} \right) \sin(kx + \alpha_k - \phi) dt \\
& + \sum_{k'} \Omega_{k'} \int_{t+(i-1)\Delta\tau_C}^{t+i\Delta\tau_C} \sin(k'x + \alpha_{k'} - \phi) dt \sum_k \Omega_k \int_{t+(i-1)\Delta\tau_C}^{t+i\Delta\tau_C} (k\Delta x - \Delta\phi) \cos(kx + \alpha_k - \phi) dt . \quad (22)
\end{aligned}$$

Then we replace the left hand of (19b) with the right hand side of (22) and the right hand side of (19b) with the right hand side of (14a) and exploit the random phase approximation to produce

$$\frac{\Delta\tau_C^2}{2} \sum_k \Omega_k^2 \left[1 - \frac{\langle (k\Delta x - \Delta\phi)^2 \rangle}{2} \right] = \frac{\cos^2 \theta}{\sin^2 \theta} \frac{\Delta\tau_C^4}{4^2} \left(\sum_k \Omega_k^2 \right)^2 . \quad (23)$$

Condition (23) must be consistent with the stochastic differential equations of motion (16). The latter can be directly integrated over an auto-correlation time since the dependent variables θ , ϕ , and x do not change significantly over $\Delta\tau_C$. Thus, equations (16) require that

$$k\Delta x - \Delta\phi = kV_o \cos\theta \Delta\tau_C + \Omega_o \Delta\tau_C - \sqrt{\frac{\Delta\tau_C^2 \cos^2 \theta}{2 \sin^2 \theta} \sum_k \Omega_k^2} N_{\phi,t}(0,1) \quad (24)$$

from which the result

$$\langle (k\Delta x - \Delta\phi)^2 \rangle = (kV_o \cos\theta + \Omega_o)^2 \Delta\tau_C^2 + \frac{\Delta\tau_C^2 \cos^2\theta}{2 \sin^2\theta} \sum_k \Omega_k^2, \quad (25)$$

follows immediately. Note that (25) is correct through second order in $\Delta\tau_C$.

Using (25) to eliminate $\langle (k\Delta x - \Delta\phi)^2 \rangle$ from (23) and solving for the auto-correlation time $\Delta\tau_C$ produces

$$\Delta\tau_C = \frac{\sqrt{2}}{\sqrt{(kV_o \cos\theta + \Omega_o)^2 + \frac{3 \cos^2\theta}{4 \sin^2\theta} \sum_k \Omega_k^2}} \quad (26)$$

where here the overbar indicates a wave energy density weighted average

$$\overline{(kV_o \cos\theta + \Omega_o)^2} = \frac{\sum_k \Omega_k^2 (kV_o \cos\theta + \Omega_o)^2}{\sum_k \Omega_k^2}. \quad (27)$$

Result (26) also follows, in similar fashion, from the alternative but equivalent necessary condition $\langle Z_i(t, \Delta\tau_C) Z_{i+1}(t, \Delta\tau_C) \rangle = \langle Z_i(t, \Delta\tau_C) \rangle \langle Z_{i+1}(t, \Delta\tau_C) \rangle$.

Equation (26) indicates that the auto-correlation time $\Delta\tau_C$ is, as suggested earlier, a relatively complicated function of the pitch angle θ , the background field amplitude Ω_o , and the spectrum of wave amplitudes Ω_k . When $\Delta\tau_C$ is eliminated from expression (17b) for the diffusion rate D we arrive at

$$D = \frac{\sum_k \Omega_k^2 / \sqrt{2}}{\sqrt{(kV_o \cos \theta + \Omega_o)^2 + \frac{3 \cos^2 \theta}{4 \sin^2 \theta} \sum_k \Omega_k^2}}. \quad (28)$$

Therefore, the diffusion rate D is also a function of the pitch angle θ , the background field amplitude Ω_o , and the spectrum of wave amplitudes Ω_k . These factors regulate the size of $\Delta\tau_c$ and D in the following ways.

The diffusion rate D is directly proportional to the wave energy density $\sum_k \Omega_k^2$ for relatively small $\sum_k \Omega_k^2$ -- a result that is consistent with quasi-linear theory [1, 23].

However, when the wave energy density and pitch angle are such that

$\frac{3 \cos^2 \theta}{4 \sin^2 \theta} \sum_k \Omega_k^2 \gg \overline{(kV_o \cos \theta + \Omega_o)^2}$, the diffusion rate becomes proportional to the square

root of the wave energy density, that is, $D \propto \frac{\sin \theta}{\cos \theta} \sqrt{\sum_k \Omega_k^2}$. This dependence, one not

reproduced by standard quasi-linear theory, is especially important near the loss cone of trapped particles where pitch angles are small.

The size of the positive definite term $\overline{(kV_o \cos \theta + \Omega_o)^2}$ in (26) and (28) depends on whether or not the wave amplitudes are strongly peaked or not and whether or not the particles are resonant with the waves at this peak. When wave spectra are strongly peaked at wave number k_o the term $\overline{(kV_o \cos \theta + \Omega_o)^2} \approx (k_o V_o \cos \theta + \Omega_o)^2$. Particles with speed V_o and pitch angle θ that satisfy $k_o V_o \cos \theta + \Omega_o \approx 0$ are said to be resonant with the wave k_o . Therefore, the auto-correlation time and diffusion rate are relatively large

for particles resonant with highly peaked spectra and relatively small otherwise. Wave spectra that are broad rather than peaked do not exhibit this behavior.

These features are quantitatively illustrated when the spectral wave energy density Ω_k^2 is a continuous function of k proportional to a Gaussian wave number distribution $\exp[-(k - k_o)^2 / 2\Delta k^2]$ with mean k_o and (standard deviation) width Δk . In this case

$$\overline{(kV_o \cos\theta + \Omega_o)^2} = (\Delta k V_o \cos\theta)^2 + (k_o V_o \cos\theta + \Omega_o)^2 . \quad (29)$$

This factor is a minimum, and thus $\Delta\tau_c$ and D are, according to (26) and (28), near maximum whenever the particle pitch angle θ is related to the mean wave number k_o by the resonance condition

$$k_o V_o \cos\theta + \Omega_o = 0 , \quad (30)$$

a condition met for electrons ($\Omega_o = -\Omega_{oe} < 0$) with a pitch angles $0 \leq \theta < \pi/2$ and for positive ions ($\Omega_o = \Omega_{oi} > 0$) with pitch angles $\pi/2 < \theta \leq \pi$.

V. Physical Limitations

We have made three assumptions in deriving expressions for the stochastic differential equations of motion (16) and their consequences: the random variable, the two-time scale, and the random phase assumptions. By requiring that the stochastic

equations of motion (16) and their consequences be consistent with these assumptions we uncover the physical parameter range for which equations (16) are valid.

The random phase approximation is always consistent with the stochastic differential equations of motion (16) because the right hand sides of the equations of motion (16b) and (16c) for the dependent variables x and ϕ are themselves independent of x and ϕ . Therefore, if the random variable $kx + \alpha_k - \phi$ is at any time uniformly distributed, it will remain so because there is no tendency in (16) for $kx + \alpha_k - \phi$ to bunch.

On the other hand, the random variable and two-time scale assumptions require, respectively, that a correlation time $\Delta\tau_c$ exist and that it be small compared to the time required for the dependent variables to change significantly. This latter time is quantified, according to (16a), with the drift and diffusion times C^{-1} and D^{-1} . Because the diffusion time D^{-1} restricts the relative wave energy density ε , that is, restricts

$$\varepsilon = \frac{\sum_k \Omega_k^2}{\Omega_o^2}, \quad (31)$$

more than does the drift time C^{-1} , the random variable and two-time scale assumptions reduce to the single condition $\Delta\tau_c D \ll 1$, which, given (26) and (28), is equivalent to

$$\varepsilon \ll \left(\frac{kV_o \cos \theta}{\Omega_o} + 1 \right)^2 + \frac{3 \cos^2 \theta}{4 \sin^2 \theta} \varepsilon. \quad (32a)$$

When the wave energy spectrum is distributed continuously in a Gaussian with mean k_o and width Δk condition (32a) becomes

$$\varepsilon \ll \left(\frac{\Delta k V_o \cos \theta}{\Omega_o} \right)^2 + \left(\frac{k_o V_o \cos \theta}{\Omega_o} + 1 \right)^2 + \frac{3 \cos^2 \theta}{4 \sin^2 \theta} \varepsilon . \quad (32b)$$

According to conditions (32), the angle at which $(3 \cos^2 \theta)/(4 \sin^2 \theta) = 1$ defines a critical pitch angle $\theta_c = \tan^{-1} \sqrt{3/4} \approx 41^\circ$ much below which the stochastic equations of motion (16) are valid for any relative wave energy ε . Alternatively, for pitch angles θ much above the critical angle $\theta_c \approx 41^\circ$ the validity of equations (16) is limited to the regime for which

$$\varepsilon \ll \left(\frac{k V_o \cos \theta}{\Omega_o} + 1 \right)^2 \quad (33a)$$

or equivalently

$$\varepsilon \ll \left(\frac{\Delta k V_o \cos \theta}{\Omega_o} \right)^2 + \left(\frac{k_o V_o \cos \theta}{\Omega_o} + 1 \right)^2 . \quad (33b)$$

Evidently, the theory is most severely constrained for large pitch angle particles resonant with highly peaked spectra.

VI. Test Particle Simulations

We solve the deterministic equations of motion (5) for a series of non-interacting electrons. This series of solutions constitutes one test particle simulation. The charged particles in any one test particle simulation are initialized with the same pitch angle θ_o and with random initial position x_o and phase ϕ_o uniformly distributed, respectively, over the largest wavelength and the interval $[0, 2\pi]$. Also the electrons in a test particle simulation interact with the same spectrum of wave amplitudes.

Because we simulate electrons, $\Omega_o = -\Omega_{oe}$ where $\Omega_{oe} = eB_o/\gamma_o m_e$ is the (positive definite) relativistic electron cyclotron frequency. Therefore, the normalized auto-correlation time $\Delta\tau_c \Omega_{oe}$ and diffusion rate D/Ω_{oe} become, according to (26) and (28)

$$\Delta\tau_c \Omega_{oe} = \frac{\sqrt{2}}{\sqrt{\left(\frac{kV_o}{\Omega_{oe}} \cos\theta - 1\right)^2 + \frac{3 \cos^2 \theta}{4 \sin^2 \theta} \epsilon}} \quad (34a)$$

and

$$\frac{D}{\Omega_{oe}} = \frac{\epsilon/\sqrt{2}}{\sqrt{\left(\frac{kV_o}{\Omega_{oe}} \cos\theta - 1\right)^2 + \frac{3 \cos^2 \theta}{4 \sin^2 \theta} \epsilon}} \quad (34b)$$

The test particle simulations illustrate and test the accuracy of expressions (34a) and (34b). The right hand sides of (34a) and (34b) depend upon the shape of the wave

spectrum with which the electrons interact as well as upon the electron pitch angle θ and the relative wave energy density ε . We simulate two shapes. The first spectrum is flat; the second is Gaussian-shaped. In each test particle simulation we plot the variance of the pitch angle $\langle \theta^2 \rangle - \langle \theta \rangle^2$ versus normalized time $\Omega_{oe} t$. After a brief period during which the variance grows as t^2 , the variance begins to grow as t . This linear growth rate is the normalized diffusion constant D/Ω_{oe} as long as the magnitude of the variance stays very small compared to its equilibrium value ($\approx 1/2$). The normalized auto-correlation time $\Delta\tau_c \Omega_{oe}$ is closely correlated with the duration of initial parabolic growth. Sometimes, the linear growth phase of the variance is followed by oscillations in the variance especially if the particles are not resonant with any of the prescribed waves.

Flat Spectrum. In this case the wave field amplitudes are uniform, that is, $\Omega_k = \Omega_w > 0$, for n_w wave numbers between minimum and maximum values, respectively, k_{\min} and k_{\max} . The normalized wave numbers are $kV_o/\Omega_{oe} = (1, 2, \dots, n_w)/(n_w \cos \theta_{\max})$ with maximum $k_{\max} V_o/\Omega_{oe} = 1/\cos \theta_{\max}$ and minimum $k_{\min} V_o/\Omega_{oe} = 1/(n_w \cos \theta_{\max})$ where the angle θ_{\max} is a convenient way to parameterize k_{\max} and k_{\min} and an indication of the maximum pitch angle $\cos^{-1}[1/(k_{\max} V_o/\Omega_{oe})]$ at which particles can resonate with a wave. When the number of waves is large, that is, when $n_w \gg 1$, equations (34) reduce to

$$\Delta\tau_c \Omega_{oe} = \frac{\sqrt{6}}{\sqrt{\left(\frac{\cos \theta}{\cos \theta_{\max}}\right)^2 - 3\left(\frac{\cos \theta}{\cos \theta_{\max}}\right) + 3 + \varepsilon \frac{9 \cos^2 \theta}{4 \sin^2 \theta}}} \quad (35a)$$

and

$$\frac{D}{\Omega_{oe}} = \frac{\varepsilon\sqrt{3/2}}{\sqrt{\left(\frac{\cos\theta}{\cos\theta_{\max}}\right)^2 - 3\left(\frac{\cos\theta}{\cos\theta_{\max}}\right) + 3 + \varepsilon\frac{9\cos^2\theta}{4\sin^2\theta}}}. \quad (35b)$$

Figures (1a)-(1c) display features of the time evolution of the pitch angle variance $\langle\theta^2\rangle - \langle\theta\rangle^2$ of 1000 particles with initial pitch angle $\theta_o = 20^\circ$. These particles scatter from a flat spectrum of 100 magnetic waves with relative energy $\varepsilon = 0.001$ and wave numbers parameterized by a maximum resonant pitch angle $\theta_{\max} = 80^\circ$. One component of the wave magnetic field with random uniformly distributed wave phase angles α_k is shown in Figure (1a). The root mean square magnetic field strength is recognizably close to $\sqrt{\varepsilon} = \sqrt{0.001} \approx 0.0316$. Figure (1b) shows the pitch angle variance $\langle\theta^2\rangle - \langle\theta\rangle^2$ as a function of normalized time $t\Omega_{oe}$. Initially when the variance $\langle\theta^2\rangle - \langle\theta\rangle^2$ grows as t^2 the particles are still evolving deterministically from their initial conditions. The duration of this deterministic growth phase corresponds closely to the auto-correlation time as determined by (35a), that is, for these parameters it corresponds closely to $\Delta\tau_c\Omega_{oe} = 0.611$. The normalized diffusion rate D/Ω_{oe} for these parameters is determined numerically from this graph and others like it by fitting a straight line to the variance's linear growth phase. Its slope ($5.2 \cdot 10^{-4}$) is reasonably close to that ($3.1 \cdot 10^{-4}$) predicted by equation (35b). A histogram showing the pitch angle distribution at the end of the evolution shown in Figure (1b), that is, at $t\Omega_{oe} = 1.5$, is shown in Figure (1c). In

this and other test particle simulations particle pitch angles are not allowed to evolve very far from their initial value.

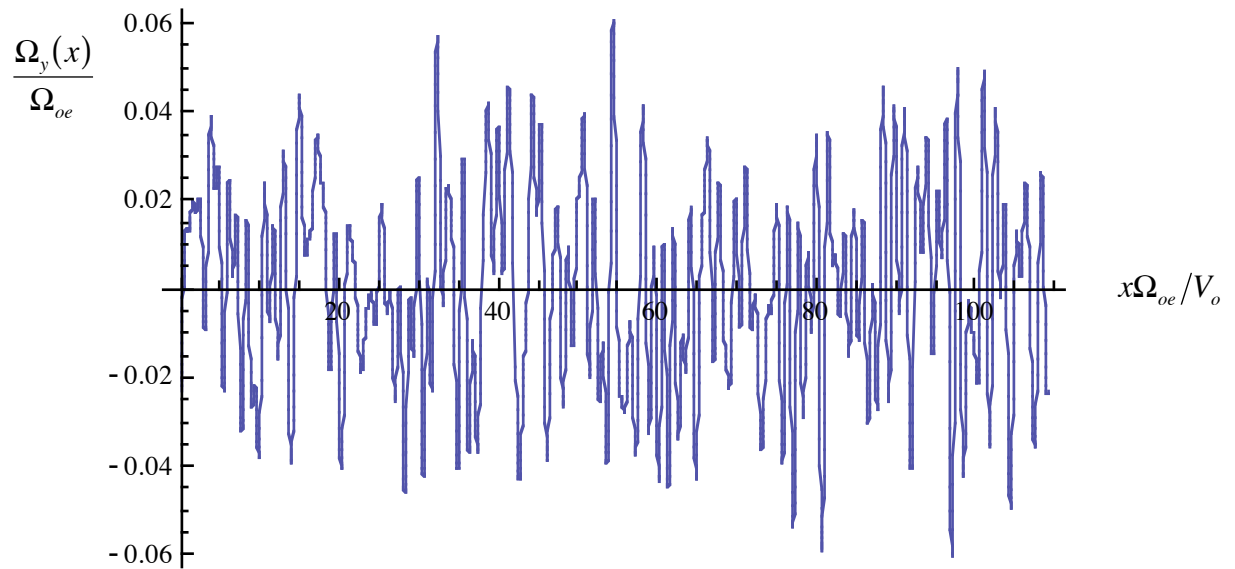


Figure (1a). One component of the normalized magnetic field composed of 100 equal magnitude waves over the longest wavelength for relative wave energy $\varepsilon = 0.001$ and spectral parameter $\theta_{\max} = 80^\circ$.

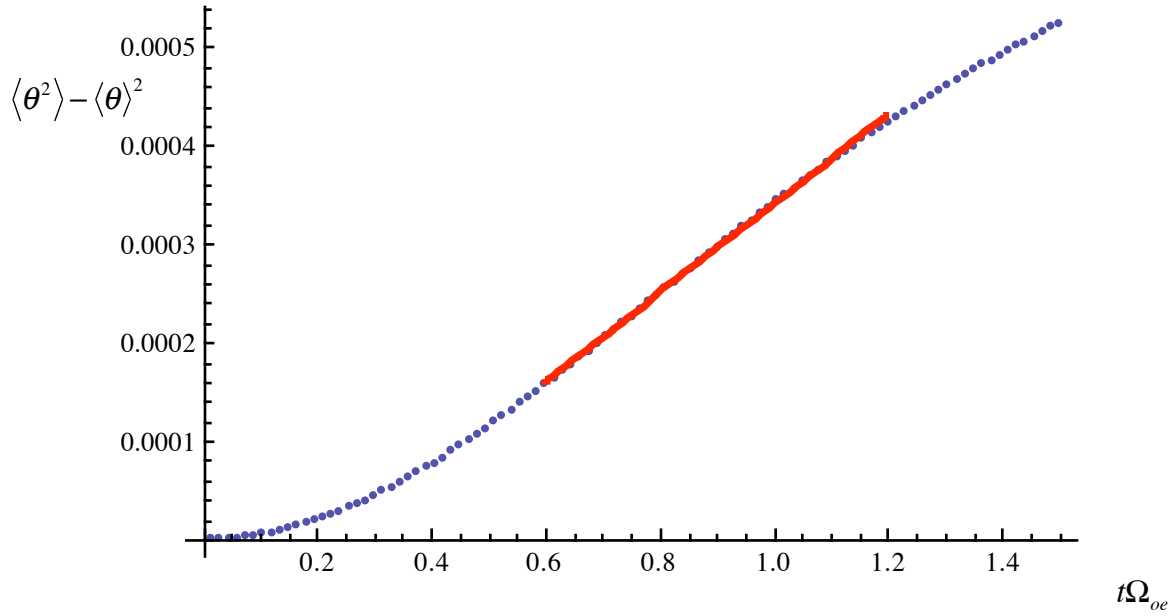


Figure (1b). Particle variance $\langle \theta^2 \rangle - \langle \theta \rangle^2$ as a function of normalized time $t\Omega_{oe}$ for 1000 particles with initial pitch angle $\theta_o = 20^\circ$ interacting with 100 equal magnitude waves of relative wave energy density $\varepsilon = 0.001$ and spectral parameter $\theta_{\max} = 80^\circ$. The slope of the straight line superimposed on the linear growth phase is the normalized diffusion rate

$$D/\Omega_{oe}$$

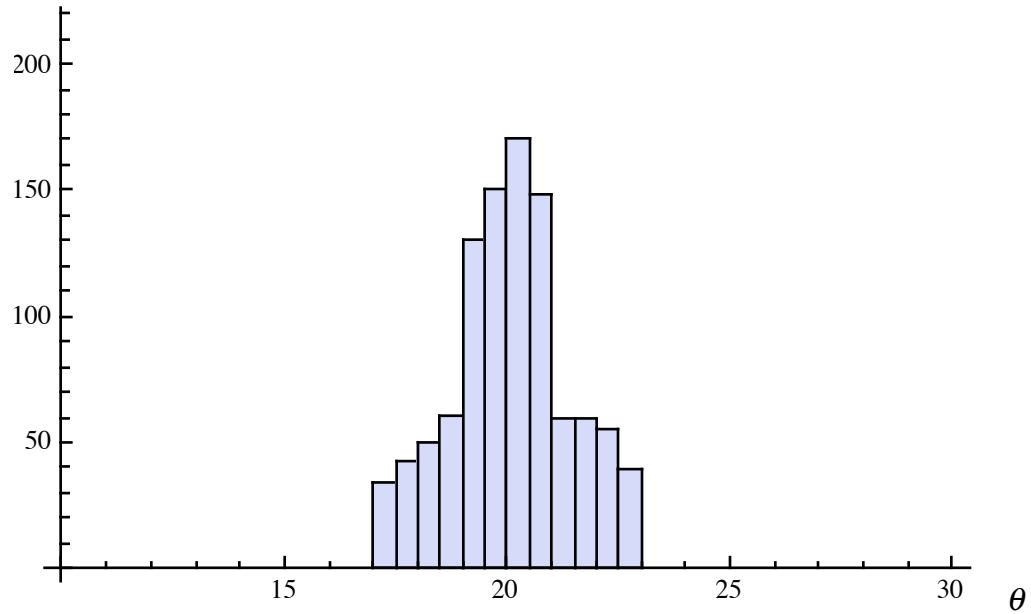


Figure 1c. Histogram of 1000 particles in pitch angle space at the end of the period shown in Figure 1b, that is, at $t\Omega_{oe} = 1.5$.

Figure 2 shows the normalized diffusion rate D/Ω_{oe} as a function of initial pitch angle θ_o as the latter varies from 0° to 180° . The particles interact with 100 equal magnitude waves of relative wave energy $\varepsilon = 0.001$ and spectral parameter $\theta_{\max} = 80^\circ$. The solid line is the diffusion constant as determined by (35b). The diffusion constant extracted from a single 200 test particle simulation varies as much as 100% with the particular realization of the set of uniform random variables x_o and ϕ_o . For this reason

we average the diffusion constant extracted from three 200 test particle simulations of the deterministic equations of motion (5) in order to produce the filled circles. The simulations reproduce the magnitude and structure expected fairly well.

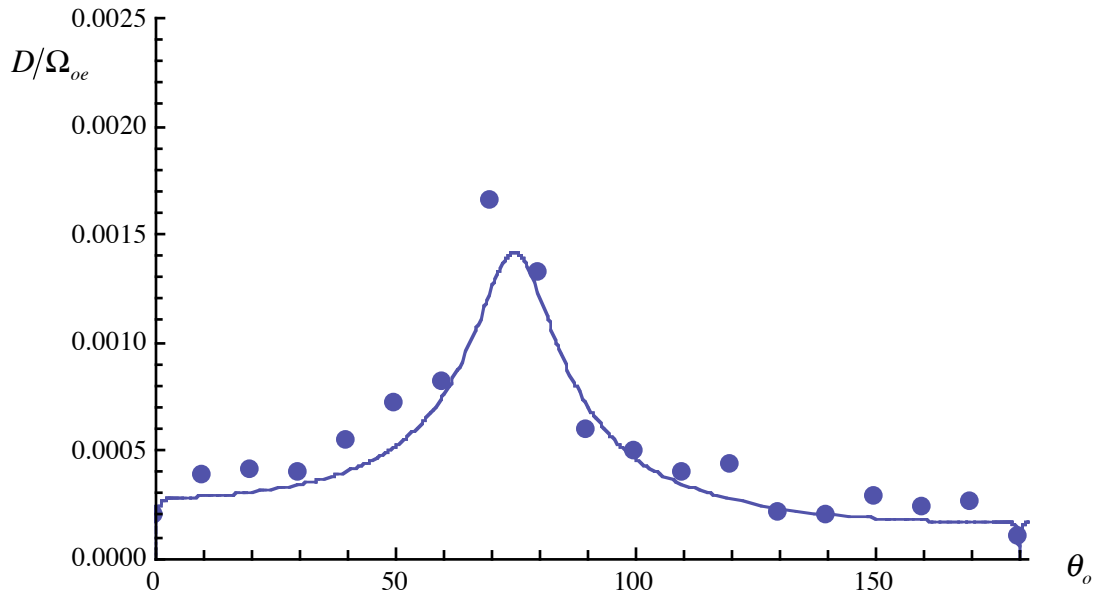


Figure 2. Normalized diffusion rate D/Ω_{oe} versus initial pitch angle θ_o for interaction with a flat spectrum of 100 waves parameterized by $\theta_{\max} = 80^\circ$ with relative energy $\varepsilon = 0.001$. The solid curve is determined from (35b). Each filled circle is the average of three numerical diffusion rates extracted from 200 test particle solutions of the deterministic equations of motion (5).

Figure 3 shows the normalized diffusion rate D/Ω_{oe} for initial pitch angle $\theta_o = 15^\circ$ and interaction with 100 equal magnitude waves parameterized by $\theta_{\max} = 80^\circ$

and relative wave energy densities ε ranging from 10^{-4} to 10^2 . The solid curve is D/Ω_{oe} determined by (35b) for these parameters. The filled circles are the average diffusion rate extracted from three 200 test particle numerical solutions of the deterministic equations of motion (5) for these parameters. As expected, the theoretical description remains fairly accurate even for wave energy densities much larger than the background field energy density.

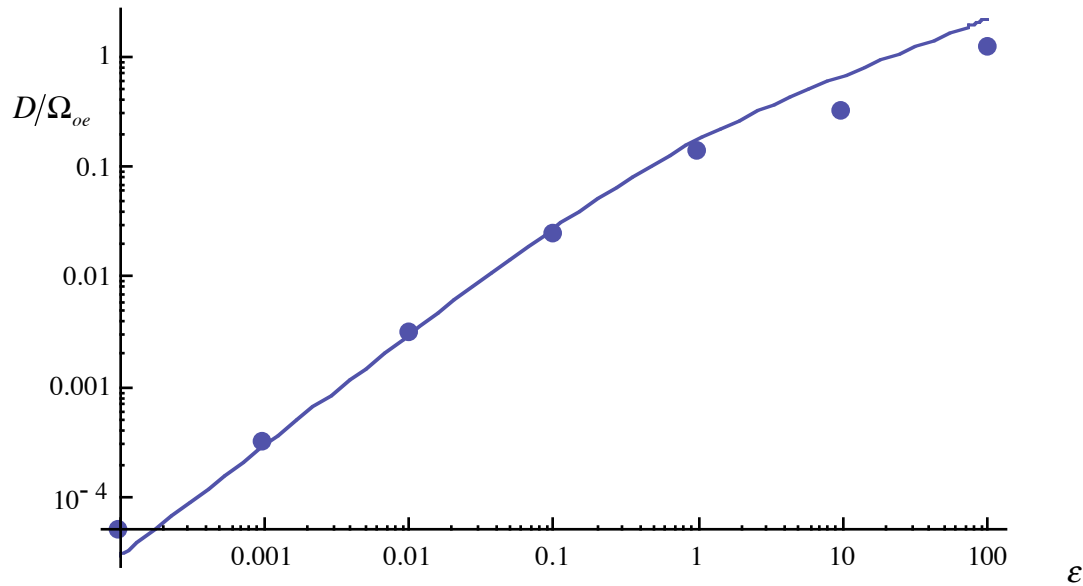


Figure 3. Normalized diffusion rate D/Ω_{oe} for initial pitch angle $\theta_o = 15^\circ$ and interaction with 100 equal magnitude waves parameterized by $\theta_{\max} = 80^\circ$ as a function of relative wave energy ε ranging from 10^{-4} to 10^2 . The solid curve is determined from equation (35b) while the filled circles are calculated from three 200 test particle numerical solutions of the deterministic equations of motion (5).

Figure 4 shows the normalized diffusion rate D/Ω_{oe} for particles with initial pitch angle $\theta_o = 90^\circ$ interacting with a flat spectrum of 100 waves with spectral parameter $\theta_{\max} = 80^\circ$ versus relative wave energy ε . The solid curve is D/Ω_{oe} as determined by (35b) for these parameters. In this case expressions (35) give a simple result:

$\Delta\tau_c\Omega_{oe} = \sqrt{2}$, $D/\Omega_{oe} \approx \varepsilon/\sqrt{2}$, and thus $D\Delta\tau_c = \varepsilon$. Therefore, when $\varepsilon \geq 1$, $D\Delta\tau_c \geq 1$ and the theoretical model should fail. Indeed, the numerical diffusion rate calculated from the average of three 200 test particle solutions of the deterministic equations of motion (5) falls short by more than factor of ten below that predicted by (35b) when $\varepsilon = 100$.

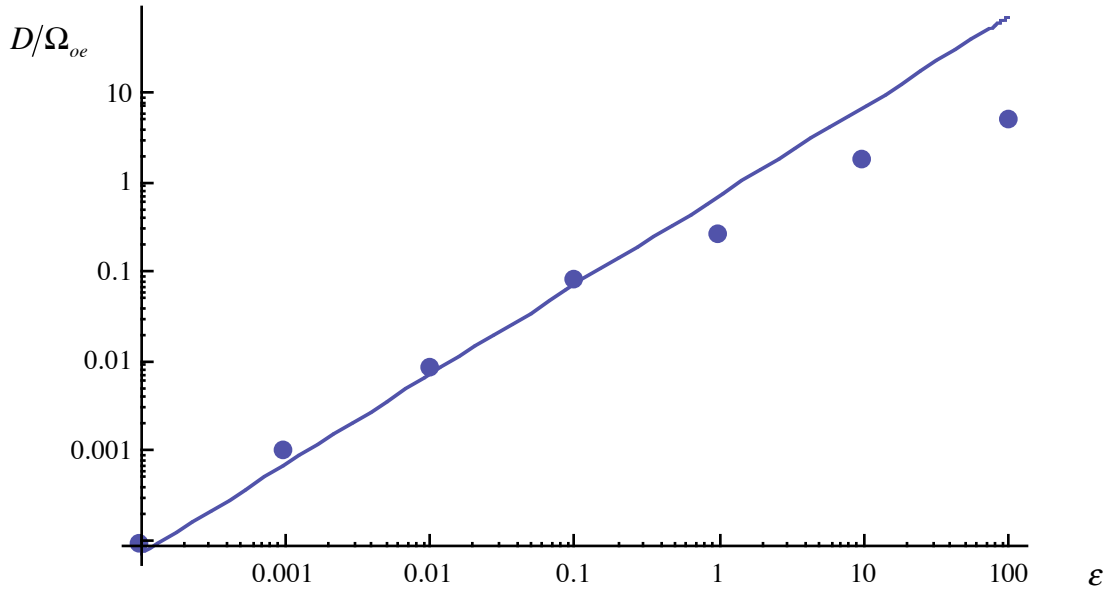


Figure 4. Normalized diffusion rate D/Ω_{oe} as a function of relative wave energy ϵ for initial pitch angle $\theta_o = 90^\circ$ and spectral properties $\theta_{\max} = 80^\circ$ and $n_w = 100$. The solid curve is determined by equation (35b) while the filled circles are the diffusion rate D/Ω_{oe} averaged over three 200 test particle solutions of the deterministic equations of motion (5).

Gaussian Spectrum. In this case the waves have a spectral energy density Ω_k^2 proportional to $\exp[-(k - k_o)^2 / 2\Delta k^2]$ with n_w discrete wave numbers evenly spaced between a minimum k_{\min} and a maximum k_{\max} . To parameterize this distribution we, somewhat arbitrarily, choose a discrete Gaussian wave spectrum with four-sigma domain,

that is, one for which $k_{\max} - k_{\min} = 4\Delta k$ centered on the mean or peak wave number k_o .

This parameterization allows us to select the wave number at peak spectral energy density k_o and the smallest wave number k_{\min} and from these calculate the other parameters, that is, $k_{\max} = 2k_o - k_{\min}$ and $\Delta k = (k_o - k_{\min})/2$. Accordingly, the normalized wave numbers are

$kV_o/\Omega_{oe} = (k_{\min}V_o/\Omega_{oe}) + (0,1,2,\dots,n_w)(2/n_w)[(k_oV_o/\Omega_{oe}) - (k_{\min}V_o/\Omega_{oe})]$. If the wave numbers k were distributed continuously over an infinite interval, the auto-correlation time and the diffusion rate would be given by

$$\Delta\tau_c\Omega_{oe} = \frac{\sqrt{2}}{\sqrt{\left(\frac{\Delta k V_o}{\Omega_{oe}} \cos\theta\right)^2 + \left(\frac{k_o V_o}{\Omega_{oe}} \cos\theta - 1\right)^2 + \frac{3 \cos^2\theta}{4 \sin^2\theta} \varepsilon}} \quad (36a)$$

and

$$\frac{D}{\Omega_{oe}} = \frac{\varepsilon/\sqrt{2}}{\sqrt{\left(\frac{\Delta k V_o}{\Omega_{oe}} \cos\theta\right)^2 + \left(\frac{k_o V_o}{\Omega_{oe}} \cos\theta - 1\right)^2 + \frac{3 \cos^2\theta}{4 \sin^2\theta} \varepsilon}} \quad (36b)$$

Since the waves are actually discretely distributed over a finite range, equations (36) are only approximate.

Figure 5 shows the diffusion rate caused by 100 waves distributed as a Gaussian with $k_{\min}V_o/\Omega_{oe} = 1.0$ and $k_oV_o/\Omega_{oe} = 3.0$. Therefore, $\Delta kV_o/\Omega_{oe} = 1.0$ and $k_{\max}V_o/\Omega_{oe} = 5.0$. These choices make the largest amplitude waves resonant with

particles at pitch angle 71° and the whole four-sigma spectrum of waves resonant with particles with pitch angles between 0° and 78° . The solid line is the diffusion rate as determined by (36b). The filled circles are the numerically determined diffusion rate averaged over three 200 test particle solutions of the deterministic equations of motion (5). In all these simulations the relative wave energy is $\varepsilon = 0.01$. The numerical results are noisy but roughly match the magnitude and structure expected from equation (36b).

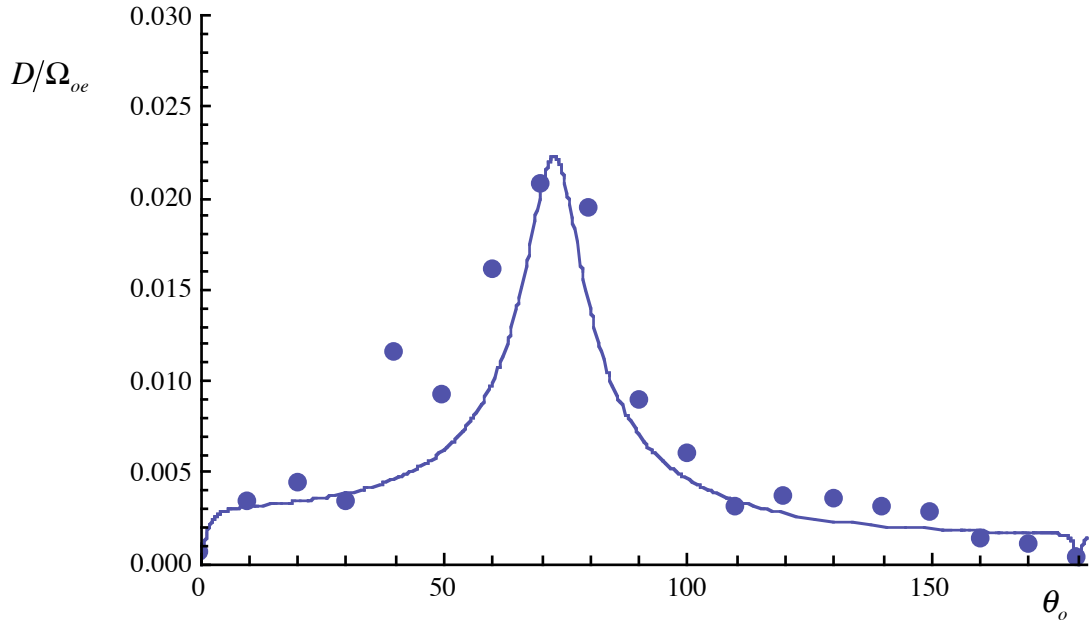


Figure 5. Normalized diffusion rate D/Ω_{oe} as a function of initial pitch angle θ_o for particles interacting with 100 waves with relative wave energy $\varepsilon = 0.01$ and spectral energy density proportional to a four-sigma Gaussian with mean $k_o V_o / \Omega_{oe} = 3.0$, minimum $k_{\min} V_o / \Omega_{oe} = 1.0$, maximum $k_{\max} V_o / \Omega_{oe} = 5.0$, and (standard deviation) width $\Delta k V_o / \Omega_{oe} = 1.0$. The solid line is determined from the relation (36b). Filled circles are averaged over three 200 test particle solutions of the deterministic equations of motion (5).

VII. Conclusion

We have derived a theory of the pitch angle scattering of charged particles from a static magnetic field composed of a background field and a sum of transverse, circularly polarized, magnetic waves. The derivation starts with the deterministic equations of motion (5) and makes those approximations – the random variable, the two-time scale,

and the random phase approximation – necessary to transform them into stochastic differential equations (16). From the latter we extract an expression (28) for the pitch angle diffusion rate D that is a function of the pitch angle θ , the background field amplitude Ω_o , the wave energy density $\sum_k \Omega_k^2$, and the shape of the wave amplitude spectrum Ω_k . This function remains valid for wave energy densities $\sum_k \Omega_k^2$ up to 100 times larger than the energy density of the background field Ω_o^2 when the pitch angle is much smaller than 41° . Also this function is convergent for resonant particles and for particles with 90° pitch angles. These features distinguish the current stochastic theory from usual implementations of quasi-linear theory.

We have also performed several sets of grid-less test particle simulations in which the particles are initialized with a specific pitch angle and uniformly distributed random positions and phases. The particles interact with a prescribed, static configuration of transverse, circularly polarized, magnetic waves. These simulations support the theory fairly well.

This kind of scattering has also been treated extensively by quasi-linear theory [21-24] and, more recently, by test particle simulations that use spectra of low-frequency waves derived analytically [25] and from self-consistent plasma simulations [26]. Both approaches lead to expressions for the pitch angle scattering rate of energetic electrons. A future challenge of the present stochastic approach is to more directly compare its predictions with these others.

We also anticipate extending the stochastic theory to describe inelastic wave-particle interactions. Relativistic electrons trapped in the earth's magnetosphere do, in

fact, interact with relatively high frequency, transverse, whistler waves [25, 35]. In this case the effect of the wave electric field must be included in the analysis and, as a result, particle energy diffusion competes with pitch angle diffusion. We expect that the random variable, the two-time scale, and the random phase approximations will apply in this case and that a similar analysis will yield similarly useful results.

In this paper we have, in order to validate the current stochastic theory, emphasized the initial value problem in which all the test particles are initialized with the same pitch angle. Ultimately, we want to apply this theory to the problem of pitch angle scattering into the loss cone of high-energy, relativistic electrons trapped in the earth's magnetic field. But this scattering usually occurs in the context of a steady state pitch angle distribution. Therefore, future application of these methods and results to scattering into the loss cone should emphasize a steady state initial distribution more typical of magnetospheric conditions.

ACKNOWLEDGMENT This work was performed under the auspices of the U.S. Department of Energy (DOE). It was supported primarily by the Defense Threat Reduction Agency under the "Basic Research for Combating Weapons of Mass Destruction (WMD)" Program, project IACRO # 07-4323I, with additional support from the Heliospheric Guest Investigators Program of the National Aeronautics and Space Administration.

References

-
1. Dröge, W., "Particle scattering by magnetic fields," *Space Science Rev.* **93**, 121-151 (2000).
 2. Millan, R. M., and R. M. Thorne, "Review of radiation belt relativistic electron losses," *J. Atmos. Sol-Terr. Phys.* **69**, 362-377 (2007).
 3. Gary, S. P., *Theory of Space Plasma Microinstabilities* (Cambridge, 1993) pp. 106-112.
 4. Thorne, R. M., and C. F. Kennel, "Relativistic electron precipitation during magnetic storm phase," *J. Geophys. Res.* **76**, 4446 (1971).
 5. Inan, U. S., T. F. Bell, and R. A. Hellliwell, "Nonlinear pitch angle scattering of energetic electrons by coherent VLF waves in the magnetosphere," *J. Geophys. Res.* **83**, 3235 (1978).
 6. Lorentzen, K. R., M. P. McCarthy, G. K. Parks, J. E. Foat, R. M. Millan, D. M. Smith, R. P. Lin, and J. P. Treilhou, "Precipitation of relativistic electrons by interaction with electromagnetic ion cyclotron waves," *J. Geophys. Res.*, **105**, A3. 5381-5389 (2000).
 7. Green, J. C., T. G. Onsager, T. P. O'Brien, and D. N. Baker, "Testing loss mechanisms capable of rapidly depleting relativistic electron flux in the Earth's outer radiation belt," *J. Geophys. Res.*, **109**, A12211, doi:10.1029/2004JA010579 (2004).
 8. Bortnik, J., R. M. Thorne, T. P. O'Brien, R. J. Strangeway, Y. Y. Shprits, and D. N. Baker, "Observation of two distinct, rapid loss mechanisms during the 20 November 2003 radiation belt dropout event," *J. Geophys. Res.* **111**, A12216, doi:10.1029/2006JA011802 (2006).

-
9. Shprits, Y. Y., D. A. Subbotin, N. P. Meredith, and S. R. Elkington, "Review of modeling losses and sources of relativistic electrons in the out radiation belt II: Local acceleration and loss," *J. Atmos. Sol. Terr. Phys.* **70**, 1694, doi:10.1016/j.jastp.2008.06.014 (2008).
 10. Shprits, Y. Y., L. Chen, and R. M. Thorne, "Simulations of pitch angle scattering of relativistic electrons with MLT-dependent diffusion coefficients," *J. Geophys. Res.* **114**, A03219, doi:10.1029/2008JA013695 (2009).
 11. Jordanova, V. K., J. Albert, and Y. Miyoshi, "Relativistic electron precipitation by EMIC waves from self-consistent global simulations," *J. Geophys. Res.* **113**, A00A10, doi:10.1029/2008JA013239 (2008).
 12. Anderson, B. J., and D. C. Hamilton, "Electromagnetic ion cyclotron waves stimulated by modest magnetospheric compressions," *J. of Geophys. Res.*, **98**, 11369-82 (1993).
 13. Anderson, B. J., R. E. Denton, G. Ho, D. C. Hamilton, and S. A. Fuselier, and R. J. Strangeway, "Observational test of local proton cyclotron instability in the Earth's magnetosphere," *J. Geophys. Res.* **101**, 21,527-21,543 (1996).
 14. Meredith, N. P., R. M. Thorne, R. B. Horne, D. Summers, B. J. Fraser, and R. R. Anderson, "Statistical analysis of relativistic electron energies for cyclotron resonance with EMIC waves observed on CRRES," *J. Geophys. Res.* **108**, 1250, doi:10.1029/2007JA012368 (2003).
 15. Mauk, B. H., and R. L. McPherron, "An experimental test of the electromagnetic ion cyclotron instability within the Earth's magnetosphere," *Phys. Fluids* **23**, 211-227 (1980).

-
16. Erlandson, R. E. and A. J. Ukhorskiy, "Observations of electromagnetic ion cyclotron waves during geomagnetic storms: Wave occurrence and pitch angle scattering," *J. Geophys. Res.* **106**(A3), 3883-3895 (2002).
 17. Miyoshi, Y., and R. Kataoka, "Ring current ions and radiation belt electrons during geomagnetic storms driven by coronal mass ejections and corotating interaction regions," *Geophys. Res. Lett.* **32**, L21105, doi:10.1029/2005GL024590 (2005).
 18. Kennel, C. F. and F. Engelmann, "Velocity space diffusion from weak plasma turbulence in a magnetic field," *Phys. Fluids* **9**, 2377 (1966).
 19. Sagdeev, R. Z, and A. A. Galeev, Nonlinear Plasma Theory (W. A. Benjamin, New York, 1969).
 20. Karimabadi, H., D. Krauss-Varraban, and T. Terasawa, "Physics of pitch angle scattering and velocity diffusion 1. Theory," *J. Geophys. Res.* **97**, 13,853-13,864 (1992).
 21. Steinacker, J. and J. A. Miller, "Stochastic gyroresonant electron acceleration in a low beta plasma. I. Interaction with parallel transverse cold plasma waves," *Astrophys. J.* **393**, 764-781 (1992).
 22. Albert, J. M., "Evaluation of quasi-linear diffusion coefficients for EMIC waves in a multi-species plasma," *J. Geophys. Res.* **108**, 1249, doi:10.1029/2002JA 009792 (2003).
 23. Summers, D. and R. M. Thorne, "Relativistic electron pitch-angle scattering by electromagnetic ion cyclotron waves during geomagnetic storms," *J. Geophys. Res.* **108**, 1143, doi:10.1029/2002JA009489 (2003).

-
24. Summers, D., “Quasi-linear diffusion coefficients for field-aligned electromagnetic waves with applications to the magnetosphere,” *J. Geophys. Res.* **110**, A09213, doi:10.1029/2005JA011159 (2005).
 25. Bortnik, J., R. M. Thorne, and U. S. Inan, “Nonlinear interaction of energetic electrons with large amplitude chorus,” *Geophys. Res. Lett.* **35**, L21102, doi:10.1029/2008GL03500 (2008).
 26. Liu, K. J., D. S. Lemons, D. Winske, and S. P. Gary, “Relativistic electron scattering by electromagnetic ion cyclotron fluctuations: test particle simulations,” to be submitted (2009).
 27. Lemons, D. S., *An Introduction to Stochastic Processes in Physics* (Johns Hopkins University Press, Baltimore, 2002) pp. 101-102.
 28. Gillespie, D. T. *Markov Processes: An Introduction for Physical Scientists* (Academic Press, 1992) pp. 111-122.
 29. Gary, S. P. (1993), pp. 93-95.
 30. Lemons, D. S. (2002) p. 21.
 31. Gardiner, C. W. *Handbook of Stochastic Methods* (Springer, New York, 1985) pp. 16-17.
 32. Lemons, D. S. (2002) pp. 36-39.
 33. Gillespie, D. T. (1992) pp. 35-29.
 34. Lemons, D. S. (2002) pp. 59-60.
 35. Summers, D., B. Ni, and N. P. Meredith, “Timescales for radiation belt electron acceleration and loss due to resonant wave-particle interactions: 2. Evaluation for

VLF chorus, ELF hiss, and electromagnetic ion cyclotron waves,” J. Geophys. Res.

112, A04207, doi:10.1029/2006JA011993 (2008).